^{13}C High-Pressure CPMAS NMR Characterization of the Molecular Motion of Polystyrene Plasticized by CO_2 Gas

Toshikazu Miyoshi, K. Takegoshi, and Takehiko Terao*

Department of Chemistry, Graduate School of Science, Kyoto University, Kyoto 606-01, Japan

Received December 26, 1996; Revised Manuscript Received August 19, 1997[⊗]

ABSTRACT: ^{13}C high-pressure CPMAS NMR is applied to examine the interaction between a CO_2 gas and polystyrene under CO_2 gas pressures of 0−7 MPa. The molecular motion of polystyrene at atmospheric pressure is also studied for comparison by ^{13}C CPMAS NMR in the temperature range 35−104 °C. The obtained ^{13}C CPMAS NMR spectra and ^{13}C $T^*_{1\rho}$ values show that while the interchain distances in the densely packing regions are heterogeneously expanded with increasing temperature, they are homogeneously expanded at high CO_2 gas pressures.

Introduction

So far, a great interest has been attracted in gas−polymer interactions because of the industrial and scientific importance. Permeation,[1] dilation,[2] and sorption[3] measurements have been used to study the translation of gas molecules, the volume of a polymer dilated by gas, and the amount of sorbed gas molecules, respectively. The obtained data have been interpreted by the dual-mode model. This model assumes the existence of two gas binding sites which have different affinities with gas molecules independent of gas pressure. Under high gas pressures, however, this model becomes inadequate, because the polymer structure is affected by dissolved gas molecules; they swell the polymer to increase the interchain distance[2] (the plasticization effect), leading to enhancement of the mobility of polymer. The enhancement of motion by the plasticization effect has been detected as decrease of glass transition temperature (T_g) for several glassy polymers.[4,5]

A few NMR investigations have been reported for the plasticization effect of a CO_2 gas on glassy polymers.[6,7] Sefcic *et al.* measured the ^{13}C spin−lattice relaxation time in the rotating frame ($T_{1\rho}$) of poly(vinyl chloride) (PVC) at various CO_2 gas pressures to study the molecular motion of PVC.[6] Although they observed a correlation between $T_{1\rho}$ and gas pressure, the observed change in $T_{1\rho}$ is very small because of the narrow pressure range (0−0.1 MPa). Smith *et al.* applied ^2H NMR methods to probe the effects of CO_2 gas pressure (0−5 MPa) on the molecular motion of fully deuterated polystyrene (PS).[7] From the ^2H spin−lattice relaxation time (T_1) measurements, they suggested that the frequency of local motions such as libration of the main chain and π-flip motion of the phenyl ring increases with increasing CO_2 gas pressure. In these works, gas effects on the main chain motion, which is related to the T_g of polymers, was not appreciated.

So far, ^{13}C CPMAS NMR has been used to characterize the molecular motion of solid polymers.[8] Recently, we have developed a simple method to obtain ^{13}C CPMAS spectra under high gas pressure.[9] In this study, we use this method to investigate the molecular motion enhanced by dissolved CO_2 gas as well as variable-temperature ^{13}C CPMAS to compare the CO_2 gas effects with temperature effects.

* To whom correspondence should be addressed.

[⊗] Abstract published in *Advance ACS Abstracts,* October 1, 1997.

Experimental Section

Sample. Polystyrene (PS) sample was obtained from Polyscience Co. The weight average molecular-weight (M_w) of PS mainly used in this study is 2500. PS was dissolved in benzene, casted on a Teflon plate, and dried for 1 week at room temperature. After that, we dried it under vacuum at 70 °C for 5 days. The T_g of PS was found to be 58 °C using differential scanning calorimetry (DSC) measurements with a heating rate of 5 °C/min. To examine the effects of polydispersity of molecular weight, two PS samples (M_w = 5000 and 9000) with a monodispersity of M_w/M_n < 1.1 were obtained from Aldrich Chemical Co. All the NMR measurements have been done for the sample with M_w = 2500 unless otherwise denoted.

High-Pressure MAS. High-pressure magic-angle spinning (MAS) was realized as follows: A Pyrex glass tube containing a sample, whose inside and outside diameters are 3.40 and 5.85 mm, respectively, was attached to a vacuum line and degassed. After that, the CO_2 gas, which is enough to give a required pressure, was transferred into the glass tube immersed in a liquid N_2 bath; then, the glass tube was sealed off. The sealed glass tube was inserted into a Chemagnetics 7.5 mm MAS spinner with powdered glass or KBr to well balance the spinner. Further details are described in ref 9.

NMR Measurements. We performed the experiments using a Chemagnetics CMX-300 NMR spectrometer operating at 300.5 MHz for protons. The radiofrequency field strength is about 55.6 kHz for either ^1H or ^{13}C. The contact time of cross-polarization (CP) was usually set to 1 ms. Under pressures above 3 MPa or at temperatures above T_g, however, the ^{13}C $T_{1\rho}$ becomes short, and then the CP contact time of 0.5 ms was used. The frequency of MAS rate was set to 4.5 kHz. Variable-temperature experiments were performed in the range 35−104 °C. The measurements of ^{13}C CPMAS NMR spectra and relaxation times under CO_2 gas pressures were made at 35 °C.

Results and Discussion

Temperature Effect. Figure 1 shows ^{13}C CPMAS NMR spectra measured at 35, 87, and 104 °C under atmospheric pressure. The signal at 40 ppm is a superposition of the methine and methylene resonances, which can be fitted with two Gaussian line shapes; the higher and lower field peaks can be assigned to the methine and methylene carbons, respectively (Figure

S0024-9297(96)01891-8 CCC: $14.00

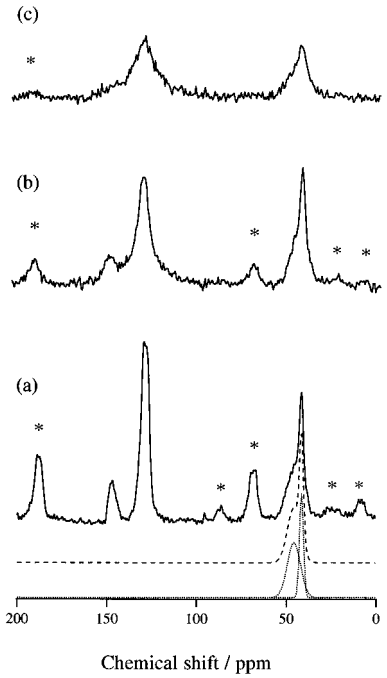

Figure 1. ^{13}C CPMAS NMR spectra of polystyrene: (a) 35 °C; (b) 87 °C; (c) 104 °C. The broken and the dotted lines represent the overlapped and the separated signals, respectively, calculated for the aliphatic carbons using two Gaussian line shapes. The higher and lower field peaks are assigned to the methine and methylene carbons, respectively.

1a).[10] Those at 127 and 145 ppm are ascribed to the protonated and nonprotonated aromatic carbons, respectively. With increasing temperature, both aromatic carbon peaks show line-broadening and the spinning sideband intensities decrease (Figure 1b), and a further increment of temperature brings about line-broadening of the main-chain carbon peaks as well as further broadening of the aromatic carbon peaks (Figure 1c). The line-broadening under ^1H dipolar decoupling (DD) and MAS can be brought about by the interference between motional narrowing and artificial narrowing due to DD[11,12] or MAS.[13] The line-broadening of the main-chain carbon having strong $^{13}C-^1H$ dipolar interactions arises mainly from the interference between motional narrowing and DD. In the aromatic carbons, which have large chemical shift anisotropies, the interference between motion and MAS may contribute to the line-broadening. The protonated aromatic carbon broadens also by the interference between motion and DD. Therefore, the protonated aromatic carbon peak is slightly broader than the nonprotonated aromatic carbon (Figure 1b). The decrease of the sideband intensities is also caused by motional averaging of the chemical shift anisotoropies of the aromatic carbons. These observations indicate that the molecular motion of PS is 1−60 kHz at these temperatures.

To further examine the molecular motion of PS, we measured the ^{13}C spin−lattice relaxation time in the rotating frame ($T_{1\rho}$) of the methine and protonated aromatic carbons at various temperatures. $T_{1\rho}$ is sensitive to the motion whose frequency is close to the spin-locking field strength (55.6 kHz). While $T_{1\rho}$ of ^1H spins in solids is unified by spin-diffusion, the $T_{1\rho}$ values of different carbons are not averaged, because the low natural abundance of ^{13}C spins inhibits spin diffusion. This makes ^{13}C $T_{1\rho}$ measurements useful to study the molecular dynamics of each functional group in polymers.

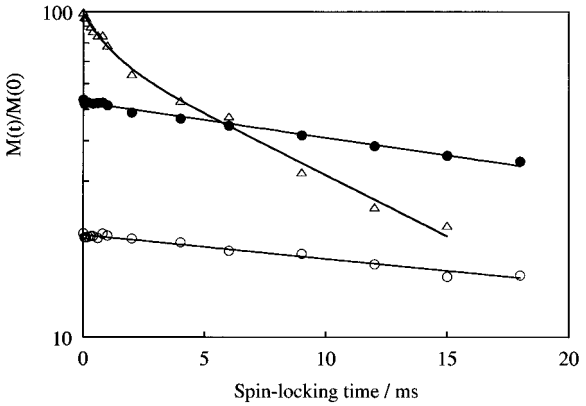

Figure 2. ^{13}C $T^*_{1\rho}$ relaxation curves of the methine carbon at various temperatures: (○) 35 °C; (●) 56 °C; (△) 77 °C. For the sake of visual clarity, data are displaced vertically.

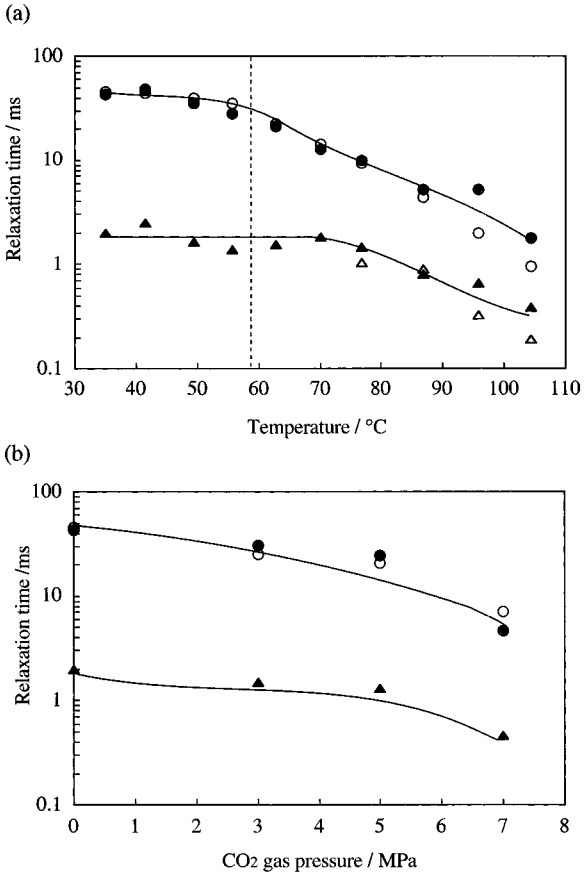

Figure 3. Temperature (a) and pressure (b) dependences of $T^*_{1\rho}$ values for the methine (○, △) and protonated aromatic (●, ▲) carbons in polystyrene. The circle and triangle represent the longer and shorter components of $T^*_{1\rho}$ values, respectively. The dashed line represents the T_g of polystyrene. The solid lines are only to guide the eye.

Figure 2 shows the $T^*_{1\rho}$ relaxation curves observed for the methine carbon at three temperatures ($T^*_{1\rho}$ is explained below). The relaxation curves observed for the methine carbon at 35 and 56 °C are fitted to a single exponential curve, and that at 77 °C is fitted to a double-exponential curve. On the other hand, all the $T^*_{1\rho}$ curves observed for the protonated aromatic carbon are fitted to a double-exponential curve. The temperature dependence of the $T^*_{1\rho}$ and the component ratio of the shorter $T^*_{1\rho}$ for the methine and protonated aromatic carbons are shown in Figures 3a and 4a, respectively.

Several possibilities are invoked to explain the observed nonexponential $T^*_{1\rho}$ decay. In fact, a $T^*_{1\rho}$ decay

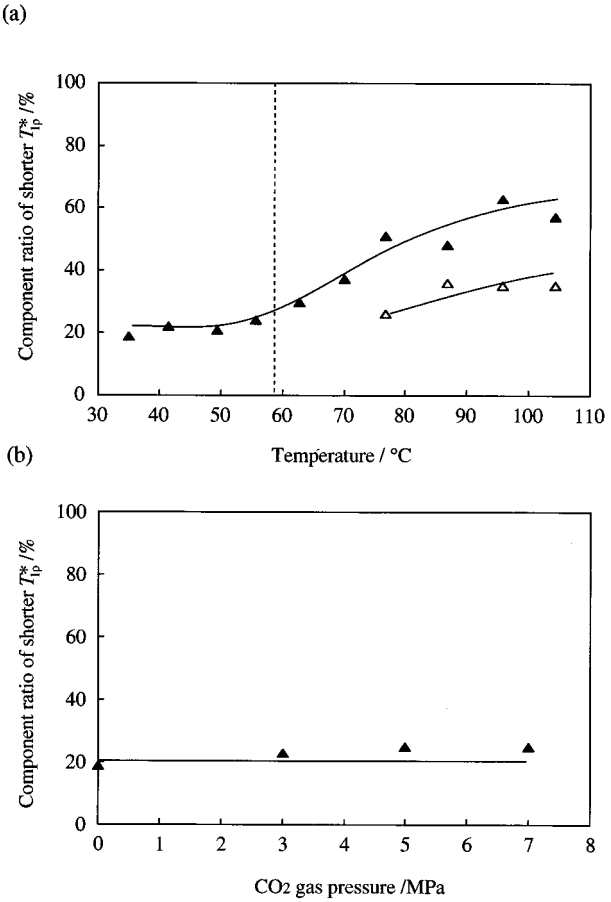

Figure 4. Temperature (a) and pressure (b) dependences of the component ratio of the shorter $T^*_{1\rho}$ in polystyrene. △ and ▲ represent the component ratios of shorter $T^*_{1\rho}$ for the methine and protonated aromatic carbons, respectively.

is intrinsically double-exponential, because fluctuation of the dipolar coupling between the ^{13}C spins and the ^1H spins is caused by two mechanisms: the molecular motion and the flip-flop motion of ^1H spins. Thus, one has to consider two thermal reservoirs, namely, the ^{13}C rotating-frame Zeeman reservoir and the ^1H dipolar reservoir, which are coupled with the lattice with different characteristic relaxation times, $T_{1\rho}$ and $T_{1D}{}^H$, respectively. These two reservoirs are coupled to each other with a characteristic time T_{CH}, leading to a double-exponential $T^*_{1\rho}$ decay. However, it has been shown[14] that, under MAS conditions, the ^1H dipolar reservoir quickly goes to the state equilibrium with the lattice ($T_{1D}{}^H \ll T_{CH}$). In this case, it can be shown that the ^{13}C rotating-frame Zeeman reservoir relaxes single-exponentially with an effective relaxation time $T^*_{1\rho}$:[14]

$$\frac{1}{T^*_{1\rho}} = \frac{1}{T_{1\rho}} + \frac{1}{T_{CH}} \qquad (1)$$

Therefore, the observed double-exponential decays show that at least two $T^*_{1\rho}$ values exist in PS. Surely several explanations for the $T^*_{1\rho}$ dispersions are possible and can be invoked as follows: (1) conformational and/or chain packing[15] heterogeneity; (2) polydispersity of molecular weight; (3) motional heterogeneity[16] between central and end regions in one polymer chain.

To examine the origin of the double-exponential decays, we further measured $T^*_{1\rho}$ decay curves for the protonated aromatic carbons of two monodispersive ($M_w/M_n < 1.1$) PS samples with different molecular weights of (a) $M_w = 5000$ and (b) $M_w = 9000$ at room temperature. Also in these samples, two $T^*_{1\rho}$ components were observed for the protonated aromatic carbons with $T^*_{1\rho}$ values of (a) 1.2 ± 0.2 and 37.0 ± 2.5 ms and (b) 1.5 ± 0.2 and 40.0 ± 2.1 ms. These values are almost in agreement with those observed for the PS sample with $M_w = 2500$ (1.8 ± 0.4 and 43.0 ± 2.7 ms). Further, the component ratio of the shorter value is (a) 17% and (b) 18%; the values agree with that of 18% for the PS sample with $M_w = 2500$. Thus, the longer and shorter $T^*_{1\rho}$ and the component ratio are concluded to be virtually independent of M_w. Therefore, it is clear that the nonexponential behavior for the protonated aromatic carbon does not come from the polydispersity of molecular weight. Furthermore, the motional heterogeneity between the center and end groups is also excluded because even with increasing M_w, the shorter $T^*_{1\rho}$ component ratio is unchanged in spite of the decrease of the end region ratio.

Measurements of ^2H spectra of PS with the deuterated phenyl ring (PS-d_5) showed that ^2H spectrum consists of a narrow and a broad line shape below T_g (80 °C).[15] The former narrow component was attributed to the phenyl ring flipping with a frequency of 10^{-7}–10^{-8} s, while the broad one was assigned to the rigid phenyl ring. The flipping and the rigid phenyl rings were assigned to those in the loosely and closely chain packing regions, respectively. In a ^{13}C T_1 measurement at room temperature,[10] a double-exponential decay was observed for the protonated aromatic carbon, in which the short component was attributed to the phenyl ring flipping in the loosely packing region. These results tempt one to conclude that the observed short $T^*_{1\rho}$ component of the protonated aromatic carbon is ascribed to the flipping phenyl ring. However, since the frequency of the flipping motion is too fast to shorten the $T^*_{1\rho}$, it is unlikely that the flipping motion is responsible for $T^*_{1\rho}$.

Linder *et al.* examined temperature dependence of the ^1H $T_{1\rho}$ of PS-d_3, PS-d_5, and PS-d_0 in the range from −150 to +230 °C.[17] They found that all the $T_{1\rho}$ minima occur around T_g +45 °C, while $T_{1\rho}$ values of PS-d_3 and PS-d_0 are an order of magnitude shorter than that of PS-d_5 below T_g, and they concluded that, below T_g, the amplitude of the phenyl ring libration is much larger than that of the chain vibration, their correlation times being of the same order of magnitude.[17] Therefore, we can ascribe the shorter ^{13}C $T^*_{1\rho}$ component observed below T_g for the protonated aromatic carbon to the phenyl ring libration associated with the main chain vibration in the loosely packing region. The absence of the shorter $T^*_{1\rho}$ component below T_g for the methine carbon suggests that the main-chain vibrational amplitude is too small to be appreciable by $T^*_{1\rho}$ below T_g. Above T_g, segmental motion occurring in the loosely packing region shortens $T^*_{1\rho}$ of the protonated aromatic as well as methine carbons, giving the similarly short $T^*_{1\rho}$ components of both carbons as shown in Figure 3a. The longer $T^*_{1\rho}$ components observed below and above T_g for both carbons can be assigned to the main chain vibration largely restricted in the closely packing region. They show almost the same temperature dependence of $T^*_{1\rho}$ (Figure 3a), and also the ^2H line shape for the rigid component of the phenyl ring shows a temperature dependence similar to that of the main chain above T_g,[15] so that vibrational amplitudes in the closely packing region can be considered to have little difference between the main and the side chains.

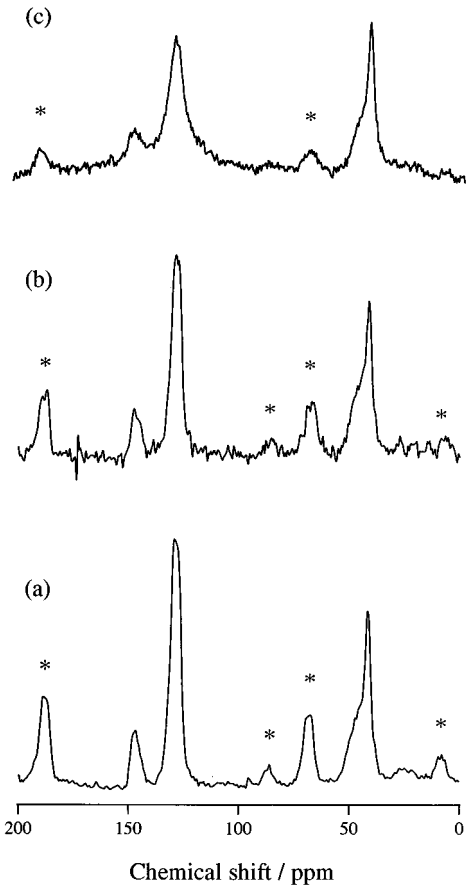

Figure 5. ^{13}C CPMAS NMR spectra of polystyrene under (a) atmospheric pressure and at CO_2 gas pressures of (b) 3 MPa and (c) 7 MPa. The signals marked by an asterisk denote the spinning sidebands for the aromatic carbons.

CO_2 Gas Pressure Effect. Figure 5 shows the pressure dependence of the ^{13}C CPMAS NMR spectrum of PS ($M_w = 2500$). A line-broadening is discernible for both the protonated and nonprotonated aromatic carbons, and the spectrum obtained under 7 MPa resembles that observed at 87 °C (Figure 1b). These observations show that molecular motion is altered by the dissolved CO_2 gas molecules. To examine the CO_2 gas pressure effect, we further measured $T^*_{1\rho}$ of PS at various CO_2 gas pressures. At all pressures examined, the $T^*_{1\rho}$ decay of the methine carbon could be expressed by a single-exponential decay curve, and that of the protonated aromatic carbon could be expressed by a double-exponential. The obtained $T^*_{1\rho}$ and the component ratio of the shorter $T^*_{1\rho}$ for the methine and the protonated aromatic carbons are shown in Figures 3b and 4b, respectively. For both carbons, the $T^*_{1\rho}$ decrease with increasing CO_2 gas pressure. For the methine carbon, the $T^*_{1\rho}$ at 3 MPa, 5 MPa, and 7 MPa roughly correspond to the longer $T^*_{1\rho}$ observed at about 60 °C, 68 °C, and 87 °C, respectively, and for the protonated aromatic carbon, the longer $T^*_{1\rho}$ at 3, 5, and 7 MPa to those at 55, 60, and 88 °C, respectively. These results show that the main-chain motion is enhanced not only by raising the temperature but also by dissolving a CO_2 gas in it.

The temperature and the CO_2 gas pressure dependence of the component ratio of the shorter $T^*_{1\rho}$ shown in Figure 4 are different from each other. Particularly, the methine carbon shows no component with shorter $T^*_{1\rho}$ even at a CO_2 gas pressure of 7 MPa, while the observed longer $T^*_{1\rho}$ at 87 °C corresponding to that at 7 MPa has the component with shorter $T^*_{1\rho}$. Also for the protonated aromatic carbon, the $T^*_{1\rho}$ component ratio shows appreciable temperature dependence, while it stays constant for the pressure range studied.

We explain the observed temperature and CO_2 gas pressure effects as follows: at temperatures higher than T_g densely packing regions are partially loosen, so that the component ratio of the shorter $T^*_{1\rho}$ (Figure 4a) increases. On the other hand, in CO_2 gas experiment, it is true that the CO_2 gas enhances motion with increasing CO_2 gas pressure (the plasticized effect), but the CO_2 gas does not change the ratio of the densely packing and the loosely packing regions (Figure 4b). Therefore, the interchain distances of the densely packing regions are heterogeneousely expanded with increasing temperature; that is, some regions are loosened but some regions are not; on the other hand, they are homogeneously expanded with increasing pressure. This homogenization effect of CO_2 gas molecules may be attributed to the fast diffusion of dissolved CO_2 gas molecules (1.0×10^{-7} cm^2/s at 2 MPa):[7] the collision of CO_2 gas molecules with PS at various sites expands the interchain distances and homogenize the heterogeneous packing structure.

Acknowledgment. This research was supported by a grant-in-aid from the Ministry of Education, Science, and Culture of Japan and a grant from the Schimadzu Science Foundation. The authors would like to thank Dr. Asano at the National Defense Academy for the DSC measurement of PS.

References and Notes

(1) (a) Barbari, T. A.; Koros, W. J.; Paul, D. R. *J. Polym. Sci., Polym. Phys. Ed.* **1988**, *26*, 709. (b) Jordan, S. M.; Koros, W. J. *J. Polym. Sci., Polym. Phys. Ed.* **1990**, *28*, 795.

(2) (a) Sefcik, D. M. *J. Polym. Sci., Polym. Phys. Ed.* **1986**, *24*, 935. (b) Sefcic, D. M. *J. Polym. Sci., Polym. Phys. Ed.* **1986**, *24*, 957. (c) Fleming, G. K.; Koros, W. J. *Macromolecules* **1986**, *19*, 2285.

(3) (a) Patel, K; Manley, R. St. J. *Macromolecules* **1995**, *28*, 5793. (b) Kamiya, Y.; Hirose, T.; Naito, Y.; Mizoguchi, K.; *J. Polym. Sci., Polym. Phys. Ed.* **1986**, *24*, 2107.

(4) Wang, V, W.; Krammer, J. E.; Sachse, J. *J. Polym. Sci., Polym. Phys. Ed.* **1982**, *20*, 1371.

(5) Hachisuka, H.; Sato, T.; Imai, T.; Tsujita, Y.; Takizawa, A.; Kinoshita, T.; *Polym. J.* **1990**, *22*, 77.

(6) Sefcik, D. M.; Shaefer, J. *J. Polym. Sci, Polym. Phys. Ed.* **1983**, *21*, 1055.

(7) Smith, B. P.; Moll, J. D. *Macromolecules* **1990**, *23*, 3250.

(8) Komoroski, R. A. *High Resolution NMR spectroscopy of synthetic polymers in Bulk*; VCH: Deerfield Beach, FL, 1986.

(9) Miyoshi, T.; Takegoshi, K.; Terao, T. *J. Magn. Reson.* **1997**, *125*, 383.

(10) Schaefer, J.; Sefcic, M. D.; McKay, R. A.; Dixon, W. T.; Cais, R. E. *Macromolecules* **1984**, *17*, 1107.

(11) VanderHart, D. L.; Earl, W. P.; Garroway, A. N. *J. Magn. Reson.* **1981**, *44*, 361.

(12) Rothwell, W. P.; Waugh, J. S. *J. Chem. Phys.* **1981**, *74*, 2721.

(13) Suwelack, D.; Rothwell, W. P.; Waugh, J. S. *J. Chem. Phys.* **1980**, *73*, 2559.

(14) VanderHart, D. L.; Garroway, A. N. *J. Chem. Phys.* **1979**, *71*, 2773.

(15) (a) Spiess. H. W. *Colloid Polym. Sci.* **1983**, *261*, 193. (b) Kulik, A. S.; Prins, K. O. *Polymer* **1993**, *34*, 4635.

(16) Kornfield, J. A.; Chung, G.-C.; Smith, S. D. *Macromolecules* **1992**, *25*, 4442.

(17) Linder, P.; Rössler, E.; Sillescu, H. *Macromol. Chem.* **1981**, *182*, 3653.

MA961891R